

Turbulent power theory in heavy-ion plasma of a Jovian magnetosphere

Vitaliy Kaminker *Geophysical Institute, University of Alaska Fairbanks, Fairbanks, Alaska 99775, USA*

(Received 24 August 2023; accepted 18 January 2024; published 13 February 2024)

Observations from various missions to Jupiter and Saturn showed that temperature of heavy-ion plasma contained in expanding discs around planets is increasing with radial distance. Magnetospheres of Jovian planets are successfully heating ions in a plasma fluid and magnetic field system. Turbulent fluctuations were suggested as a plasma heating mechanism. Suitability of turbulence to heat heavy-ion dense plasma and the source of turbulent fluctuations in Jupiter's magnetosphere is investigated. Relation between ion velocity variations and magnetic field fluctuations is derived from magnetohydrodynamic principles. This is then used to obtain turbulent power density contained in plasma fluid and magnetic field. Energy cascade in magnetohydrodynamic and kinetic subranges in different mediums is demonstrated. Measurements from magnetometer instrument on Juno mission to Jupiter are used to observe turbulent fluctuations in the magnetic field and to infer dynamics in plasma fluid. Extensive radial map of turbulent power density in Jupiter's magnetosphere inside and outside of the plasma disk is presented.

DOI: [10.1103/PhysRevFluids.9.024602](https://doi.org/10.1103/PhysRevFluids.9.024602)

I. INTRODUCTION

Jupiter's magnetosphere is a natural laboratory with highly dynamic plasma fluid and magnetic field system. Volcanic activity on Jupiter's moon Io introduces neutral gas into planet's magnetosphere at the rate of about 1 ton/s. Most of neutrals are ionized and are picked up by the planet's strong magnetic field and then move around the planet. Flowing plasma consisting mostly of heavy sulfur and oxygen ions expands radially forming a plasma disk. Observations on various missions to the giant planet showed that Jupiter's plasma disk expands nonadiabatically. Temperature of plasma is increasing with increase in radial distance. Jupiter's magnetosphere contains within a mechanism of heating plasma. One suggestion for a process of increase in ion temperature is heating of plasma fluid with turbulent fluctuations.

Turbulent power is introduced to the system at the stirring scale. It is then used to generate smaller and smaller eddies. The flow of energy is local and one way, meaning energy cascades down from larger eddies with lower frequencies to smaller eddies with higher frequencies without jumping over the frequency range [1]. Locality of energy transfer means that only the state of neighboring scales is relevant and information of stirring mechanism is eventually lost down the frequency range. This then implies some commonality of turbulent flow in different systems.

Power density in turbulent plasma flow is contained in two different mediums: variation of ion velocities in plasma fluid and fluctuations of the magnetic field. At low frequencies motion of particles is governed by MHD principles where variation in ion velocities is associated with magnetic field fluctuations. Power spectrum in this frequency subrange decays at roughly Kolmogorov rate $\propto k^{-5/3}$ or $\propto f^{-5/3}$ in frequency domain. In the kinetic subrange variations in ion velocities and magnetic fluctuations disassociate. In this subrange spectral index changes, resulting in a steeper power-law decay. These two subranges are separated by frequency of gyration of ions in the magnetic field, which is a significant marker in plasma fluid power spectrum. Aptness of turbulent fluctuations to heat plasma fluid depends on the ability of energy in ion velocity variations to cascade from larger

fluctuations in MHD subrange in to kinetic subrange so that eventually ion motion would look like temperature.

Power spectrum analysis of the time series was used to study turbulent dynamics in three-dimensional (3D) hybrid simulations to observe ion heating in Saturn and Jupiter magnetospheres [2]. A weak turbulence model was used to examine magnetic fluctuations in Jupiter's plasma disk from Galileo magnetometer measurements [3].

In this paper power density in turbulent cascade is examined to study plausibility of turbulence as a plasma fluid heating mechanism. Magnetometer measurements from Juno mission are used to observe turbulent processes in Jupiter's magnetosphere. More physically relevant model is used to describe power density in turbulent plasma flow. Relation of ion velocity variations and magnetic field fluctuations are derived in Sec. II. Energy cascade in ion fluid and magnetic field in MHD and kinetic subranges is discussed in Sec. IV. Turbulent power density is derived in Sec. V. Turbulent power observations in Jupiter's magnetosphere are presented in Sec. IX. Discussion is in Sec. X.

II. MAGNETOHYDRODYNAMIC MOMENTUM RELATION

In this work turbulence is modeled as a superposition of shear Alfvén waves. Magnetic field topology is assumed to be a steady, homogeneous main magnetic field with vanishing magnetic stress \mathbf{B}_0 , without external pressure waves and a steady-state oscillation shear Alfvén wave counter-propagating parallel to the direction of the main field $\delta\mathbf{B}_\perp = \delta\mathcal{B}_\perp e^{ik_\parallel x - i\omega t}$. Then the total magnetic field is $\mathbf{B} = \mathbf{B}_0 + \delta\mathbf{B}_\perp$.

Starting with Cauchy momentum equation, here convective derivative of the momentum equals to electromagnetic and pressure forces

$$\frac{D}{Dt}(\rho\delta\mathbf{v}) = \rho_e\mathbf{E} + \mathbf{J} \times \mathbf{B} - \nabla P.$$

In absence of external pressure waves $\frac{\partial\rho}{\partial t} = 0$ and $\nabla\rho = 0$. In addition, for steady-state oscillations $\nabla\delta v^2 = 0$. Expanding convective derivative and using Ampère-Maxwell equation for \mathbf{J}

$$\rho\frac{\partial}{\partial t}\delta\mathbf{v} - \rho\delta\mathbf{v} \times \mathbf{W} = \rho_e\delta\mathbf{E} - \frac{1}{\mu_0}\mathbf{B} \times (\nabla \times \mathbf{B}) + \epsilon_0\mathbf{B} \times \frac{\partial}{\partial t}\delta\mathbf{E} - \frac{k_B}{m_i}\rho\nabla T, \quad (1)$$

where $\mathbf{E} = \delta\mathbf{E}$ is electric field induced by magnetic field fluctuations, \mathbf{W} is vorticity of ion fluid flow, ρ is mass density, and ρ_e is charge density. For now ∇T is retained for further discussion below. Equation (1) can then be broken down in to ion motion perpendicular and parallel to the main magnetic field

$$\frac{\partial}{\partial t}\delta\mathbf{v}_\perp - \delta\mathbf{v}_\perp \times \mathbf{W} = \frac{e}{m_i}\delta\mathbf{E} - \frac{1}{\mu_0\rho}\mathbf{B} \times (\nabla \times \mathbf{B}) - \frac{i\epsilon_0\omega}{\rho}\mathbf{B}_0 \times \delta\mathbf{E} \quad (2)$$

$$\frac{\partial}{\partial t}\delta\mathbf{v}_\parallel = -\frac{i\epsilon_0\omega}{\rho}\delta\mathbf{B}_\perp \times \delta\mathbf{E} - \frac{k_B}{m_i}\nabla T. \quad (3)$$

Component of variation of velocity parallel to the main magnetic field is due to the radiation pressure $\delta\mathbf{B}_\perp \times \delta\mathbf{E}$ term generated by magnetic field fluctuation and induced electric field.

Using oscillating form of inducted electric field $\delta\mathbf{E} = \delta\mathcal{E}e^{ik_\parallel x - i\omega t}$, from Faraday's law $\delta\mathbf{E} = -\frac{\omega}{k_\parallel}\delta\mathcal{B}_\perp\hat{\mathbf{e}}'_\perp$, where $\hat{\mathbf{e}}'_\perp$ is a unit vector perpendicular to \mathbf{B}_0 , $\delta\mathbf{B}_\perp$ plane. Magnetic force density term in Eq. (2) can be expanded using identity $-\frac{1}{\mu_0}\mathbf{B} \times (\nabla \times \mathbf{B}) = \frac{1}{\mu_0}[\mathbf{B} \cdot (\nabla_\parallel + \nabla_\perp)]\mathbf{B} - \frac{1}{2\mu_0}\nabla\mathbf{B}^2$. This can then be simplified by noting that since $\mathbf{B}_0 \cdot \delta\mathbf{B}_\perp = 0$ then for steady-state oscillations the gradient of magnetic pressure vanishes $\frac{1}{2\mu_0}\nabla\mathbf{B}^2 = 0$. Also bear in mind that from assumptions on the magnetic field $(\mathbf{B}_0 \cdot \nabla_\parallel)\mathbf{B}_0 = 0$ and $(\delta\mathbf{B}_\perp \cdot \nabla_\perp)\mathbf{B}_0 = 0$. In addition from the chosen form of $\delta\mathbf{B}_\perp$, $(\delta\mathbf{B}_\perp \cdot \nabla_\perp)\delta\mathbf{B}_\perp = 0$. Then the time derivative of the fluid momentum in that direction equals to the only remaining term of the magnetic stress $(\mathbf{B}_0 \cdot \nabla_\parallel)\delta\mathbf{B}_\perp$ plus inductive terms. Equation (2)

can then be written as

$$\frac{\partial}{\partial t} \delta \mathbf{v}_{\perp} - \delta \mathbf{v}_{\perp} \times \mathbf{W} = -\frac{eB_0}{m_i} \frac{\omega}{k_{\parallel}} \frac{\delta B_{\perp}}{B_0} \hat{\mathbf{e}}'_{\perp} + iv_A^2 k_{\parallel} \frac{\delta \mathbf{B}_{\perp}}{B_0} - i \frac{\omega^2}{k_{\parallel}} \frac{v_A^2}{c^2} \frac{\delta \mathbf{B}_{\perp}}{B_0}.$$

Separating real and imaginary terms and assuming time oscillating form of velocity $\delta \mathbf{v} \propto e^{-i\omega t}$ equation of motion can be solved for velocity vector component

$$\delta \mathbf{v}_{\perp} = -v_A^2 \frac{k_{\parallel}}{\omega} \frac{\delta \mathbf{B}_{\perp}}{B_0} + \frac{v_A^2}{c^2} \frac{\omega}{k_{\parallel}} \frac{\delta \mathbf{B}_{\perp}}{B_0} \quad (4)$$

and vorticity term

$$\delta \mathbf{v}_{\perp} \times \mathbf{W} = \Omega_g \frac{\omega}{k_{\parallel}} \frac{\delta B_{\perp}}{B_0} \hat{\mathbf{e}}'_{\perp}, \quad (5)$$

where v_A is Alfvén speed, c is speed of light, and Ω_g is angular velocity of ion gyration in the magnetic field (also unfortunately known as gyrofrequency).

Motion of ions parallel to \mathbf{B}_0 from Eq. (3) can be written as

$$\frac{\partial}{\partial t} \delta \mathbf{v}_{\parallel} = -i \frac{\omega^2}{k_{\parallel}} \frac{v_A^2}{c^2} \left(\frac{\delta B_{\perp}}{B_0} \right)^2 \hat{\mathbf{e}}_{\parallel} - \frac{k_B}{m_i} \nabla_{\parallel} T.$$

For steady-state oscillations this will apply uniformly along the main magnetic field so that this term acts to increase ambient temperature rather than to generate temperature gradient. So with absence of other pressure waves along the magnetic field $\nabla_{\parallel} T = 0$. Note that $\nabla_{\parallel} \rho = 0$ and $\frac{\partial \rho}{\partial t} = 0$ still holds. So that

$$\delta \mathbf{v}_{\parallel} = \frac{v_A^2}{c^2} \frac{\omega}{k_{\parallel}} \left(\frac{\delta B_{\perp}}{B_0} \right)^2 \hat{\mathbf{e}}_{\parallel}. \quad (6)$$

In Jupiter plasma disk typically $\frac{v_A}{c} \sim 10^{-2}$ so that in the MHD limit second term of $\delta \mathbf{v}_{\perp}$ is about four orders of magnitude and $\delta \mathbf{v}_{\parallel}$ is four to six orders of magnitude smaller than the first term of $\delta \mathbf{v}_{\perp}$. In that case neglecting $\delta \mathbf{v}_{\parallel}$ and second term in $\delta \mathbf{v}_{\perp}$ is a very reasonable approximation. The motion of ions in MHD subrange then for all practical purposes become 1D oscillations associated with local magnetic field variations. Heavy-ion motion of dense plasma fluid can then be summed from magnetohydrodynamic momentum conservation as

$$\delta v_{\perp} = -v_A^2 \frac{k_{\parallel}}{\omega} \frac{\delta B_{\perp}}{B_0}. \quad (7)$$

Here note a negative sign in the ion velocity variation and magnetic field fluctuation relation. For shear Alfvén wave model with dense heavy-ion plasma result in (7) is similar to what is found in textbooks [4,5].

This picture, however, is different at very low densities when $v_A \sim c$. Then in MHD limit second term $\delta \mathbf{v}_{\perp}$ and $\delta \mathbf{v}_{\parallel}$ become comparable to the first term in $\delta \mathbf{v}_{\perp}$. So the process of converting shear motion of charged particles in to oscillating helixlike motion through inducted electric field and radiation pressure could work for electrons or maybe even for lighter ions at low densities. However, for dense heavy-ion plasma fluid frozen in condition kicks in and any transition become indiscernible. The relation of different velocity components in the kinetic subrange is discussed in more detail is Sec. VII.

III. DISPERSION AND WAVE NUMBER RELATIONS

A. Dispersion relation

In this work dispersion relation of the form similar to [6]

$$\omega^2 = k_{\parallel}^2 v_A^2 \left[1 + \left(\frac{3}{4} + \frac{T_e}{T_i} \right) k_{\perp}^2 \rho_i^2 \right]$$

is used. In this work turbulent power in heavy-ion plasma in presence of cold electrons is investigated.

$$\omega = \pm k_{\parallel} v_A \sqrt{1 + k_{\perp}^2 \rho_i^2}, \quad (8)$$

where k_{\perp} is a wave number perpendicular to the main magnetic field and ρ_i is ion gyroradius. Wave number k_{\perp} is estimated using Taylor approximation $2\pi f = k_{\perp} v \sin \theta_{vB}$ [7]. Here θ_{vB} is the angle between direction of the ion bulk velocity and the main magnetic field. In this estimate k_{\perp} is assumed to measure fluctuations that are mainly due to features moving past the instrument and ignoring fluctuations that happen in the time it takes for plasma to pass the spacecraft. This form of dispersion relation is consistent with shear Alfvén wave model derived in the reference frame of the main magnetic field used above. Comparison of oscillation features in different reference frames (spacecraft and plasma flow) is discussed in Ref. [8].

B. Wave number relation in different medium

Variations in ion velocities and fluctuations in magnetic field decouple in the kinetic subrange. It is then very possible that relations $\frac{k_{\parallel}}{k_{\perp}}$ in different media have different forms. Wave number relation due to variations in ion velocities is considered as

$$\frac{k_{\parallel}^i}{k_{\perp}} \sim \frac{\delta v_{\perp}}{v_A} = \frac{1}{\sqrt{1 + k_{\perp}^2 \rho_i^2}} \frac{\delta B_{\perp}}{B_0} \quad (9)$$

and wave number relation in power density due to fluctuations of the magnetic field is

$$\frac{k_{\parallel}^B}{k_{\perp}} \sim \frac{\delta B_{\perp}}{B_0} = \sqrt{1 + k_{\perp}^2 \rho_i^2} \frac{\delta v_{\perp}}{v_A}. \quad (10)$$

These two equations are derived from magnetohydrodynamic relation [Eq. (7)] using dispersion relation [Eq. (8)].

Dispersion relation for fluid in kinetic subrange can then be written in terms δv_{\perp} and k_{\perp} using wave number relation [Eq. (9)] as

$$\omega^i = k_{\perp} \delta v_{\perp} \sqrt{1 + k_{\perp}^2 \rho_i^2} \sim k_{\perp}^2 \delta v_{\perp} \rho_i \propto k_{\perp}^2. \quad (11)$$

Dispersion relation in the field is then written using [Eq. (10)]

$$\omega^B = k_{\perp} \delta v_{\perp} (1 + k_{\perp}^2 \rho_i^2) \sim k_{\perp}^3 \delta v_{\perp} \rho_i^2 \propto k_{\perp}^3 \quad (12)$$

so that oscillation rate and the rate of cascade of energy in kinetic subrange scales differently with the wave number in different mediums.

IV. ENERGY CASCADE IN DIFFERENT SUBRANGES

A. Energy cascade in MHD subrange

The form of the relation of energy contained in the scale associated with a wave number is inferred as a product of power laws of energy transfer rate and a wave number

$$E_k = C \epsilon^x k^y. \quad (13)$$

In MHD subrange $k_{\perp}\rho_i \ll 1$ and $\omega \sim k_{\parallel}v_A \sim k_{\perp}\delta v$. Then characteristic oscillation time of the scale l is $\tau \sim l/\delta v_{\perp}$. Energy per unit mass contained in motion is $E \sim \delta v_{\perp}^2$. Energy transfer rate between scales is $\epsilon \sim E/\tau$. Distribution of energy in wave number is $E_k = \frac{\partial E}{\partial k} \sim \delta v_{\perp}^2 l$.

Expressing Eq. (13) in quantities associated with the scale

$$\delta v_{\perp}^2 l = C \left(\delta v_{\perp}^2 \frac{\delta v_{\perp}}{l} \right)^x l^{-y},$$

where C is a dimensionless constant. Then

$$\delta v_{\perp}^2 l = C \delta v_{\perp}^{3x} l^{-x-y}.$$

Isolating power laws associated with individual variables then gives $x = 2/3$ and $y = -5/3$. In MHD subrange energy spectrum $S(k)$ cascades as $\propto k^{-5/3}$. This result is similar to what was obtained by Kolmogorov using self-similarity argument based on the universality assumed for the equilibrium range [9,10]. Note that spectrum index shallower than Kolmogorov cascade implies wave number relation $\frac{k_{\parallel}}{k_{\perp}} \propto \delta v^{\beta}$ with $\beta < 1$.

B. Energy cascade in kinetic subrange

In the kinetic subrange $k_{\perp}\rho_i \gg 1$ so that $\omega \sim k_{\parallel}v_A k_{\perp}\rho_i$. Energy per unit mass contained in fluctuations is again written as $E \sim \delta v_{\perp}^2$. This is an oversimplified estimation used to gauge power-law dependence. The energy in variations in plasma fluid and magnetic field system is contained in two different medium. As motions of magnetic field and ions decouple the amount of energy contained in fluctuations of the fluid and the field does not have to be the same. A more through treatment of energy budget in fluid and field system is presented in Sec. V.

1. Kinetic subrange cascade in plasma fluid

Estimation of oscillation time in the kinetic subrange is more involved as fluctuations in plasma fluid and magnetic field disassociate. If $\frac{k_{\parallel}}{k_{\perp}} \sim \frac{\delta v_{\perp}}{v_A}$ then oscillation time can be estimated as $\tau \sim l^2/(\delta v_{\perp}\rho_i)$ [Eqs. (9) and (11)]. Then expressing Eq. (13) in quantities associated with the scale in kinetic subrange.

$$\delta v_{\perp}^2 l = C \left(\delta v_{\perp}^2 \frac{\delta v_{\perp}\rho_i}{l^2} \right)^x l^{-y}.$$

Here cyclotron radius ρ_i does not vary with change in the size of fluctuations. Simplifying for quantities associated with the scale.

$$\delta v_{\perp}^2 l = C' \delta v_{\perp}^{3x} l^{-2x-y}.$$

Note that C' is no longer dimensionless. Then isolating power laws associated with individual variables gives $\propto k^{-7/3}$ power-law decay of energy of ion fluid velocity variations in the kinetic subrange.

2. Kinetic subrange cascade in magnetic field

On the other hand if $\frac{k_{\parallel}}{k_{\perp}} \sim \frac{\delta B_{\perp}}{B_0}$ then oscillation time is estimated as $\tau \sim l^3/\delta v_{\perp}\rho_i^2$ [Eqs. (10) and (12)]. Then expressing Eq. (13) in quantities associated with the scale in kinetic subrange.

$$\delta v_{\perp}^2 l = C \left(\delta v_{\perp}^2 \frac{\delta v_{\perp}\rho_i^2}{l^3} \right)^x l^{-y}.$$

So then a steeper decay of power spectrum in the kinetic subrange $\propto k^{-3}$ is expected. More likely is that decoupling effect is gradual and power spectrum decay in the kinetic subrange gradually changes from fluid like $\propto k^{-7/3}$ to field like $\propto k^{-3}$. Note that considering natural quantities δv_{\perp} and

l associated with motion on the scale allows to gauge power-law dependence that otherwise would not have been available using a dimensional analysis alone.

V. TURBULENT POWER DENSITY DERIVATION

A. Turbulent power density derivation

Turbulent power in dense heavy-ion plasma fluid flow is generated by variations in ion velocity δv_\perp and perpendicular fluctuations of the magnetic field δB_\perp . Total energy density is then

$$E_{\text{tot}} = E_i + E_B = \frac{1}{2} \delta v_\perp^2 + \frac{1}{2} \frac{\delta B_\perp^2}{\mu_0 \rho}. \quad (14)$$

Substituting for δv_\perp from magnetohydrodynamic momentum conservation for shear Alfvén waves [Eq. (7)] into (14).

$$E_{\text{tot}} = \frac{1}{2} \frac{\delta B_\perp^2 k_\parallel^2 v_A^4}{B_0^2 \omega^2} + \frac{1}{2} \frac{\delta B_\perp^2}{\mu_0 \rho}.$$

Transfer rate of energy between different neighboring scales is [9] $\epsilon \sim \frac{E_{\text{tot}}}{\tau} \sim E_{\text{tot}} \omega$. Total power density of the turbulent environment is then

$$q \sim \rho E_{\text{tot}} \omega \sim \frac{1}{2} \frac{\delta B_\perp^2 k_\parallel^2 v_A^4}{B_0^2 \omega} \rho + \frac{1}{2} \frac{\delta B_\perp^2}{\mu_0} \omega.$$

Substituting dispersion relation [Eq. (8)] into turbulent power density then gives

$$q \sim \frac{1}{2} \frac{\delta B_\perp^2}{B_0^2} v_A^3 k_\parallel^i \frac{\rho}{\sqrt{1 + k_\perp^2 \rho_i^2}} + \frac{1}{2} \frac{\delta B_\perp^2}{\mu_0} v_A k_\parallel^B \sqrt{1 + k_\perp^2 \rho_i^2}. \quad (15)$$

Here superscript on wave number k_\parallel^i and k_\parallel^B denotes different wave number relations in ion plasma fluid and field in the kinetic subrange. Substituting wave number relation in different medium from Eqs. (9) and (10) and using $v_A = \frac{B_0}{\sqrt{\mu_0 \rho}}$ for the Alfvén speed turbulent power density is then written as

$$q \sim \frac{1}{2} \frac{\delta B_\perp^3}{\sqrt{\mu_0^3 \rho}} k_\perp \sqrt{1 + k_\perp^2 \rho_i^2} \left[1 + \frac{1}{(1 + k_\perp^2 \rho_i^2)^{3/2}} \right]. \quad (16)$$

Then in the MHD limit $k_\perp \rho_i \ll 1$ so that

$$q_{\text{MHD}} \sim \frac{\delta B_\perp^3}{\sqrt{\mu_0^3 \rho}} k_\perp$$

the same as used in the turbulent heating model for Jupiter in Ref. [11]. In the kinetic subrange $k_\perp \rho_i \gg 1$ so that

$$q_{\text{KAW}} \sim \frac{1}{2} \frac{\delta B_\perp^3}{\sqrt{\mu_0^3 \rho}} k_\perp^2 \rho_i.$$

1. Notes on q

Equation (16) is similar to the model used in Ref. [2] to calculate turbulent heating in the Kelvin-Helmholtz simulation.

$$q' \sim \frac{1}{2} \frac{\delta B_\perp^3 k_\perp}{\sqrt{\mu_0^3 \rho}} \sqrt{1 + k_\perp^2 \rho_i^2} \left[1 + \left(\frac{1}{1 + k_\perp^2 \rho_i^2} \right) \left(\frac{1}{1 + 1.25 k_\perp^2 \rho_i^2} \right)^2 \right]. \quad (17)$$

That equation was derived using form of Walen relation [12],

$$\delta v \sim \delta v_A \left(\frac{1}{1 + k_{\perp}^2 \rho_i^2} \right)^{1/2} \left(\frac{1}{1 + 1.25 k_{\perp}^2 \rho_i^2} \right),$$

wave number relation

$$\frac{k_{\parallel}}{k_{\perp}} \sim \frac{\delta B_{\perp}}{B_0},$$

and dispersion relation similar to Eq. (8). This set of equations, however, is inconsistent with magnetohydrodynamic momentum relation [Eqs. (4) and (7)].

During the derivation of Eq. (17) in Ref. [2] q' was divided by half in the kinetic subrange. This was rationalized by turbulent power being mostly contained in the magnetic field and not in the plasma fluid at frequencies higher than the gyrofrequency. This half, however, propagated and was used in the entire range of frequencies in kinetic and in MHD subranges. Effectively turbulent power in plasma fluid was ignored in the paper dedicated to turbulent heating of ions.

2. Effect of electron population on turbulent power density

In this work turbulent power cascade in heavy-ion dense plasma in presence of cold electrons is investigated, which is a typical condition in magnetospheres of Jovian planets [13]. In principle fluctuations in the magnetic field in a heavy-ion turbulent cascade would result in electron velocity variations so that turbulent power is shared within two species. To more accurately describe particle velocity variations a system of equations would need to be considered.

$$\sum_j \frac{D}{Dt} (n_j m_j \delta \mathbf{v}_j) = \sum_j n_j e_j \delta \mathbf{E} + \mathbf{J}_j \times \mathbf{B} - \nabla P_j$$

$$\frac{1}{\mu_0} \nabla \times \mathbf{B} - \epsilon_0 \frac{\partial}{\partial t} \delta \mathbf{E} = \sum_j \mathbf{J}_j,$$

where j is a particle species.

This study also shows that to accurately describe turbulent power density in different particle species populations in all subranges, energy density relation

$$q = \frac{1}{2} \sum_j [\delta v_{\perp j}^2 + \delta v_{\parallel j}^2] \omega_j \rho_j + \frac{1}{2} \frac{\delta B_{\perp}^2}{\mu_0} \omega_j$$

should be used. Since turbulent power cascade is proportional to mass density, the contribution of electron particle motion to the total power budget will be orders of magnitude below the contribution of the ion fluid. The effect of electron motion on field fluctuations, however, needs to be more carefully considered. Here the challenge is that electrons and heavy ions would have very different gyrofrequencies.

In principle $\frac{T_e}{T_i} \gg \frac{1}{k_{\perp}^2 (f_e) \rho_i^2}$ in dispersion relation would result in different scaling of ion velocity variations and magnetic field fluctuations in both MHD and kinetic subranges. One consequence of this is that frozen-in assumption then could no longer be made at any frequency. Observation $T_e \ll T_i$ in magnetospheres of Jovian planets point to that perhaps the effect of turbulent cascade in heavy-ion plasma and magnetic field system does not result in turbulent cascade in electron population but rather manifests in a pulse like accelerations. This work, however, is outside the scope of this paper and is a subject for future study.

B. Turbulent power density inside and outside of the plasma environment

Examination of balance of turbulent power density inside and outside of the plasma disk might allow us to get an insight in the generating mechanisms of turbulent dynamics in Jupiter's magne-

tosphere. Energy cascade in the kinetic subrange is indicative of the turbulent plasma environment. However, it should be possible to compare balance of turbulent power density in and out of the plasma disk in MHD subrange. Using $\frac{k_{\parallel}}{k_{\perp}} \sim \frac{\delta v_{\perp}}{v_A} \sim \frac{\delta B_{\perp}}{B_0}$ in the MHD limit ($k_{\perp} \rho_i \ll 1$) in Eq. (15)

$$q \sim \frac{1}{2} \frac{\delta B_{\perp}^3}{B_0^3} v_A^3 k_{\perp} \rho + \frac{1}{2} \frac{\delta B_{\perp}^3}{\mu_0 B_0} v_A' k_{\perp}. \quad (18)$$

To allow for a smooth transition from inside of the plasma environment to the outside, a group velocity of the wave is used $v_A' = c / \sqrt{1 + \frac{\mu_0 \rho c^2}{B_0^2}}$.

So then as $\rho \rightarrow 0$ and $v_A' \rightarrow c$ the contribution of turbulent power from plasma fluid goes to zero and the total power becomes

$$q \rightarrow \frac{1}{2} c \frac{\delta B_{\perp}^2}{\mu_0} k_{\parallel} = \mathbf{S} \cdot \mathbf{k}_{\parallel},$$

where \mathbf{S} is a Poynting vector so that power density of the turbulent environment outside of the plasma disk describes power contained in the wave packet moving along bending main magnetic field.

VI. COUNTERPROPAGATING WAVES

Here the effect of counterpropagating waves on turbulent power in plasma fluid is described by interaction of linearly polarized plain waves. Figure 1 shows three limiting cases that differ by the angle between polarization vector. Primary effect of counterpropagating waves is that amplitudes of superposition of $\delta \mathbf{B}_{\perp}$ and $\delta \mathbf{E}$ add and subtract asymmetrically.

Expressing perpendicular, parallel velocity and vorticity in Eqs. (4), (3), and (5) in terms of $\delta \mathbf{B}_{\perp}$ and $\delta \mathbf{E}$.

$$\begin{aligned} \delta \mathbf{v}_{\perp} &= -v_A^2 \frac{k_{\parallel}}{\omega} \frac{\delta \mathbf{B}_{\perp}}{B_0} + \frac{\epsilon_0}{\rho} \mathbf{B}_0 \times \delta \mathbf{E} \\ \delta \mathbf{v}_{\perp} \times \mathbf{W} &= \frac{e}{m_i} \delta \mathbf{E} \\ \delta v_{\parallel} &= \frac{\epsilon_0}{\rho} \delta \mathbf{B}_{\perp} \times \delta \mathbf{E}. \end{aligned}$$

To emphasize the effect of counterpropagating waves limiting cases with similar amplitudes $\delta B_{\perp 1} \sim \delta B_{\perp 2}$ and no phase difference are considered.

A. Cases 1 and 2

In the first case superposition of waves with similar amplitudes results with $\delta B_{\perp} = 2\delta B_{\perp 1}$ and $\delta E \rightarrow 0$. Here $\delta \mathbf{v}_{\perp} \times \mathbf{W} \rightarrow 0$, $\delta v_{\parallel} \rightarrow 0$ and $\delta v_{\perp} = -v_A^2 \frac{k_{\parallel}}{\omega} \frac{\delta B_{\perp}}{B_0}$. This case is very similar to results

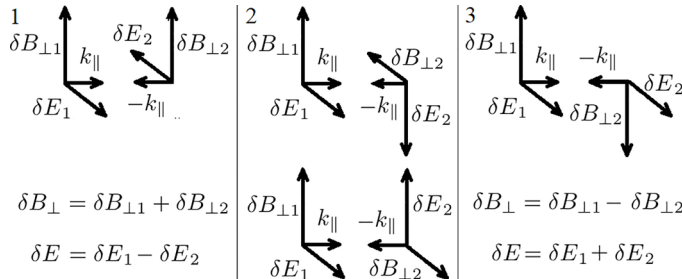


FIG. 1. Schematic of counter propagating fluctuations.

gained for the heavy-ion dense plasma $v_a \ll c$ discussed in Sec. II. Case 1 counterpropagating waves results in doubling of amplitudes of oscillations of magnetic field and variation of ion velocities. In this case correlation of ion velocities and field oscillations is expected in MHD subrange with a dissociation of velocity variations and field oscillations in kinetic subrange. In this case power is contained in the field in kinetic subrange for both dense and thin plasma fluids.

Case 2 with $\delta B_{\perp 1} \sim \delta B_{\perp 2}$ results in $\delta B_{\perp} = \sqrt{2}\delta B_{\perp 1}$ and $\delta E = \sqrt{2}\delta E_1$. Notice that since superimposed δB_{\perp} and δE are no longer perpendicular this results in $\delta v_{\parallel} \rightarrow 0$, which is consistent with cancellation of radiation pressure from two counterpropagating waves. Perpendicular velocity variations and vorticity have the same form as in Eqs. (4) and (5) with same implications for turbulent power in heavy-ion dense plasma fluid. Here it is important to note that phase difference in this case would result in elliptical polarization [5] that in principle could contribute to ion velocity variations and vorticity.

B. Case 3

Now that cases 1 and 2 are out of the way we can look at something that can be interesting. In the third case counterpropagating waves with similar amplitudes cancel out δB_{\perp} terms, isolating and doubling δE terms.

$$\begin{aligned}\delta \mathbf{v}_{\perp} &= -\frac{v_A^2}{c^2} \frac{\delta E}{B_0} \hat{\mathbf{e}}_{\perp} \\ \delta \mathbf{v}_{\perp} \times \mathbf{W} &= \frac{e}{m_i} \delta \mathbf{E}.\end{aligned}\tag{19}$$

So that in this case vorticity increases as well as perpendicular ion velocity variations in the kinetic subrange.

In this case wave number relation in ion velocity variations has the form

$$\frac{k_{\parallel}^i}{k_{\perp}} \sim \frac{\delta v_{\perp}}{v_A} = \left(\frac{v_A^2}{c^2}\right) \frac{1}{v_A} \frac{\delta E}{B_0}$$

and wave number relation in electric field variations has the form

$$\frac{k_{\parallel}^E}{k_{\perp}} \sim -\frac{1}{v_A \sqrt{1 + k_{\perp}^2 \rho_i^2}} \frac{\delta E}{B_0} = \frac{1}{\sqrt{1 + k_{\perp}^2 \rho_i^2}} \left(\frac{c^2}{v_A^2}\right) \frac{\delta v_{\perp}}{v_A}.$$

The dispersion relation for electric field fluctuations is then

$$\omega^E = k_{\perp} \frac{\delta E}{B_0} = \left(\frac{c^2}{v_A^2}\right) \delta v_{\perp} k_{\perp}.$$

Oscillation time is $\tau \sim (v_A^2/c^2)l/\delta v_{\perp}$ so that in this case spectral index in the induced electric field fluctuation is $\propto k^{-5/3}$ across the whole frequency range and no break is expected in superimposed δE power spectrum. This is the consequence of $\delta \mathbf{E} = -\frac{\omega}{k_{\parallel}} \delta B_{\perp} \hat{\mathbf{e}}'_{\perp}$ form of relation and using dispersion relation in Eq. (8) so that induced electric field fluctuations scale differently in different subranges with respect to magnetic field fluctuations.

Total energy density E_{tot} in the fluid and field system can then be expressed in terms of induced electric field fluctuations δE as

$$E_{\text{tot}} = \frac{1}{2} \left(\frac{v_A^2}{c^2}\right)^2 \frac{\delta E^2}{B_0^2} + \frac{1}{2} \frac{k_{\parallel}^2}{\omega^2} \frac{\delta E^2}{\mu_0 \rho}.$$

Then turbulent power is

$$q \sim \frac{1}{2} \left(\frac{v_A^2}{c^2} \right)^2 \frac{\delta E^2}{B_0^2} v_A \rho k_{\parallel}^i \sqrt{1 + k_{\perp}^2 \rho_i^2} + \frac{1}{2} \frac{\delta E^2 k_{\parallel}^E}{\mu_0 v_A} \frac{1}{\sqrt{1 + k_{\perp}^2 \rho_i^2}}.$$

This form is an equivalent of Eq. (15) for limiting case 3. Notice here the term that determines dynamics in the kinetic subrange $\sqrt{1 + k_{\perp}^2 \rho_i^2}$ has changed the role in fluid and the field terms. Now the turbulent power in the kinetic subrange is contained in the plasma fluid. Substituting for k_{\parallel}^i , k_{\parallel}^E , and v_A and combining we have

$$q = \frac{1}{2} \frac{\delta E^3}{B_0^3} \rho k_{\perp} \sqrt{1 + k_{\perp}^2 \rho_i^2} \left[\left(\frac{v_A^2}{c^2} \right)^3 + \frac{1}{(1 + k_{\perp}^2 \rho_i^2)^{3/2}} \right].$$

The challenge is that during the turbulent cascade counterpropagating waves would need to have opposite linear polarization over all frequency ranges from mixing scale through the kinetic subrange. Realistically it is more likely that modes will be mixed with sporadic increases and decreases of vorticity and perpendicular ion velocity variations in the kinetic subrange. In addition counterpropagating waves with similar amplitudes will negate radiation pressure variations limiting turbulent fluctuations to two dimensions.

VII. SCALING OF VELOCITY VARIATIONS, FIELD FLUCTUATIONS, AND POWER IN MHD AND KINETIC SUBRANGES

In this work dispersion relation [Eq. (8)] was used. Energy in the power spectrum needs to be conserved as it cascades from larger to lower scales in different subranges with different decay rates. The form of dispersion relation above was chosen because it scales differently in MHD ($k_{\perp} \rho_i \ll 1$) and kinetic ($k_{\perp} \rho_i \gg 1$) subranges. Note that in the MHD limit use of this choice of ω in (7) recovers Walen relation.

Turbulent power contribution from plasma fluid flow and magnetic field varies in different subranges. Interdependence of magnetic field fluctuations and ion velocity variations was shown for heavy-ion dense plasma fluid in MHD subrange from magnetohydrodynamic principles. In MHD limit fluctuations of ions in plasma fluid and magnetic field contribute equally to the turbulent power density. In the kinetic subrange velocity variations of heavy ions and magnetic fluctuations disassociate. Velocity variations scale as $\delta v_{\perp} \propto \delta B_{\perp} f^{-1}$. Contribution of turbulent fluid fluctuations to the power budget decreases with increase in frequency. In the kinetic subrange heavy-ion velocity variations rapidly decay and turbulent power is contained within magnetic field fluctuations. Increase in the decay of magnetic fluctuations is compensated by a faster rate of energy transfer between scales, so that amount of cascading energy is conserved. This way power density does not scale with frequency.

Terms in Eqs. (4) and (6) that are due to induced electric field have opposite dynamics and scale as $\propto \delta B_{\perp} f$ in the kinetic subrange. This implies that δE fluctuations are key to keeping turbulent power in the plasma in kinetic subrange. These terms, however, are also proportional to $(\frac{v_A}{c})^2$ and are only relevant in light particle, low-density plasma. Counterpropagating waves could be used to emphasize superposition of electric field fluctuations and in principle allowing us to keep turbulent power in the fluid. The difficulty is that mixed polarization of waves along the cascade will result in sporadic increases and decreases of vorticity and ion velocity variations in the kinetic subrange.

Often in the literature correlation of magnetic field fluctuations and ion velocity variations is assumed across the frequency range (critical balance argument) [14]. However, this study shows that velocity variations scale as $\delta v_{\perp} \propto \delta B_{\perp} f^{-1}$ in the kinetic subrange and critical balance argument can no longer be used.

On the other side of the spectrum is the estimate of velocity variations scaling and magnetic field fluctuations using Ampere's law [15,16]. Ampere's law, however, describes the effect of moving

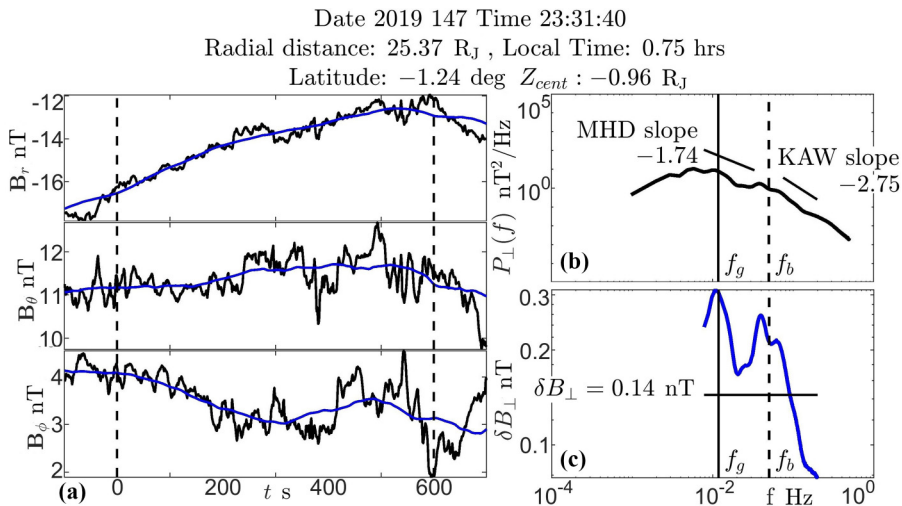


FIG. 2. (a) Radial components of magnetic field time series. Blue line is the 200 s centered moving average showing main direction of the magnetic field. Area outside dashed lines is a buffer necessary to populate moving average sliding window. Buffer zones for consecutive sampling windows overlap with neighboring sample time series to avoid data gaps. (b) Power spectrum of perpendicular fluctuations. (c) Calculated δB_\perp over sampled frequency range.

charge on the magnetic field. In order to describe the effect of magnetic field perturbations on the moving charge, force equation has to be used [5]. Use of Ampere's law results in $\delta v_\perp \propto l \delta B_\perp$ scaling across the frequency range, in MHD as well as kinetic subranges. Implying that ion velocity variations do not correlate to magnetic field fluctuations at any frequency. This was then used to estimate power spectrum cascade as $\propto k^{-7/3}$ of magnetic field fluctuations in the kinetic subrange, which was then compared to the power spectrum in the fluid velocity variations while assuming Kolmogorov $\tau \sim l/\delta v$ cascade in the fluid at the same time.

VIII. MAGNETOMETER MEASUREMENTS

A. Magnetic field fluctuations

Magnetic field fluctuations in Jupiter's magnetosphere were observed with magnetometer measurements on Juno mission to Jupiter. Juno's spacecraft polar orbit enable for comprehensive *in situ* observations of turbulent activity in Jupiter's night side magnetosphere inside and outside of the plasma disk. Location of the magnetodisc is described in terms of centrifugal equator that is derived from magnetic field topology of the tilted dipole and centrifugal forces on the plasma. Latitude off the centrifugal equator lat_{cent} is calculated as in Ref. [17] and then distance from the centrifugal equator is calculated as $Z_{\text{cent}} = r \sin(lat_{\text{sysIII}} - lat_{\text{cent}})$ [8]. Where lat_{sysIII} is latitude in planet's rotating frame [18] and r is radial distance in Jupiter radii.

Time series of the magnetic field measured by Juno spacecraft [19] were analyzed in 10 min window intervals with 1 s resolution [Fig. 2(a)]. Magnetic perturbations were observed in radial Jupiter magnetic (VIP4) coordinates [18]. The main magnetic field $\mathbf{B}_0(t)$ was calculated from moving average of the magnetometer time series (blue line in Fig. 2) [3]. Fluctuations of the magnetic field were calculated as $\delta \mathbf{B}(t) = \mathbf{B}(t) - \mathbf{B}_0(t)$. Parallel perturbations of the magnetic field were then found by $\delta \mathbf{B}(t)_\parallel = [\delta \mathbf{B}(t) \cdot \hat{\mathbf{n}}(t)] \hat{\mathbf{n}}(t)$ where $\hat{\mathbf{n}}(t)$ is a unit vector in the direction of $\mathbf{B}_0(t)$. Perpendicular perturbations were then calculated as $\delta \mathbf{B}(t)_\perp = \delta \mathbf{B}(t) - \delta \mathbf{B}(t)_\parallel$ [8].

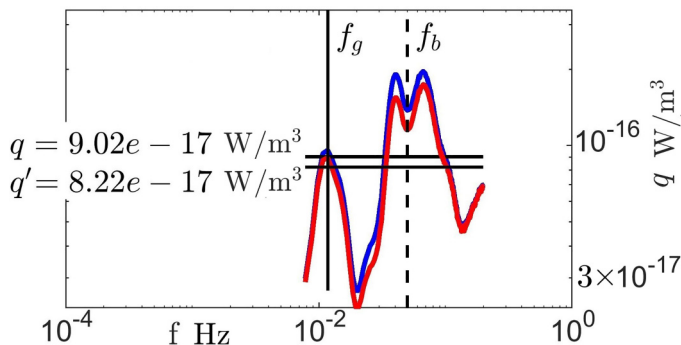


FIG. 3. Turbulent power profile as calculated by Eq. (16) (blue curve) and by Eq. (17) (red curve) from δB_{\perp} sample in Fig. 2. Horizontal lines are average of power density across the frequency range to get a value for the time series sample.

B. Power spectrum

Power spectrum is calculated from time series of $\delta \mathbf{B}_{\perp}$ components with continuous wave transform using Morlet wavelet [20]

$$P(f) = \frac{2}{N\Delta t} \sum_{i=1}^N \Delta t |W_i(t_i, f)|^2.$$

Total power density was then calculated as a square root of sum of squares of power spectrum of vector components [shown in Fig. 2(b)]. Perpendicular perturbation of the magnetic field in frequency space is calculated from the power spectrum as $(\delta B)^2 = P(f)f$ [Fig. 2(c)] [8,21,22]. Here gyrofrequency is calculated as $f_g = \frac{qB}{2\pi m_i}$. Break in the power spectrum was found by a subroutine using slope fit to the expected power-law decay [8] independently from gyrofrequency [Fig. 2(b)].

IX. TURBULENT POWER IN JUPITER'S MAGNETOSPHERE

A. Turbulent power density in plasma disk

1. Turbulent power density profile across MHD and kinetic subranges

In this study it was observed that $\frac{\delta B_{\perp} k_{\perp}}{B_0 k_{\parallel}} \sim 1$. This implies that weak turbulence is not appropriate to describe turbulent dynamics in Jupiter's magnetosphere [3]. Turbulent power spectrum profiles calculated by Eqs. q (16) and q' (17) are shown in Fig. 3. Here ion gyroradius is calculated in terms of the ion temperature $\rho_i = \frac{\sqrt{m_i k_B T_i}}{eB}$. Ion mass is an average of oxygen and sulfur masses. Bulk plasma velocity v is calculated with corotation model [13]. Temperature T and density ρ are taken from profiles in Ref. [13]. Figure 3 shows turbulent power density calculated across MHD and kinetic subranges for time series sample in Fig. 2. Overall power density profiles are very similar. Difference in the power of the denominator is not very noticeable on the log scale. A very common feature in power spectrum density profiles is an increase in turbulent power near the break frequency.

Turbulent power density measurements inside Jupiter's plasma disk are shown in Fig. 4. Range chosen is in well defined plasma disk thoroughly covered by Juno's orbit $r \in [12, 40] R_J$, $Z_{\text{cent}} \in [-2, 2] R_J$ over all sampled local time (azimuthal direction). Turbulent power for 10 min intervals is calculated as in Fig. 3 with Eq. (16). The spread of measurements is about three orders of magnitude. There is an increase of turbulent power towards the middle of the plasma disk $Z_{\text{cent}} \in [-0.5, 0.5] R_J$ with maximum values higher by about an order of magnitude than in the rest of the Z_{cent} range.

Comparison of turbulent power in MHD vs KAW subranges is shown in Fig. 5. The median is $\frac{q_{\text{KAW}}}{q_{\text{MHD}}} \sim 0.7$. In general calculated turbulent power density in different subranges are close to be

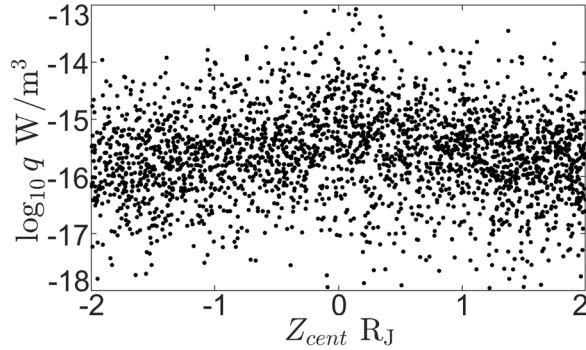


FIG. 4. Turbulent power density inside plasma disk calculated with Eq. (16).

balanced, slightly underestimating power in the kinetic subrange. This is possibly due to not using small ($\frac{v^2}{c^2}$) terms of Eqs. (4) and (6) in turbulent power calculation.

2. Cases when break in power spectrum occurs near gyrofrequency

Turbulent waves traveling in the bulk velocity plain model was used to describe the role of gyro and break frequencies in estimation of ion temperature in plasma flow [8]. Compressional and shear wave modes are mixed inside Juptier's plasma disk. Here magnetometer observations were used to see if the effect described in Ref. [8] could be seen using a shear wave turbulence model [Eq. (16)].

A common feature in power spectrum density profiles is an increase in turbulent power near break frequency of the power spectrum (Fig. 3). To demonstrate this an overplot of a subset of turbulent power profiles is shown in Fig. 6. Profiles closer to the middle of the plasma disk are chosen in $r \in [12, 40] R_J$ and $Z_{cent} \in [-1, 1] R_J$ with calculated gyro and break frequencies [Figs. 2(b), 2(c), and 3] similar to each other $\frac{f_g - f_b}{f_g} < 1$. For comparison purposes frequency was scaled by break frequency and power density was scaled by the value of power density at the break frequency for each sample. Curves are plotted opaque so that color shows density of over plotted power spectrum.

In this subset there is a peak of about an order of magnitude towards frequency of break in the power spectrum. Moreover, in these cases turbulent power is overall higher in the kinetic subrange than in MHD subrange. This demonstrates that oscillations near break and gyrofrequencies play an important role in transferring energy to plasma fluid in Jupiter's magnetosphere.

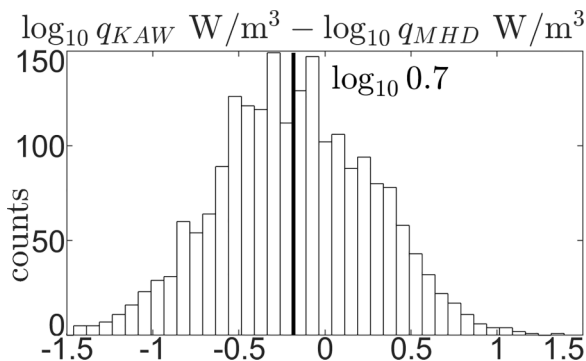


FIG. 5. Difference between turbulent power density calculated in MHD and kinetic subranges.

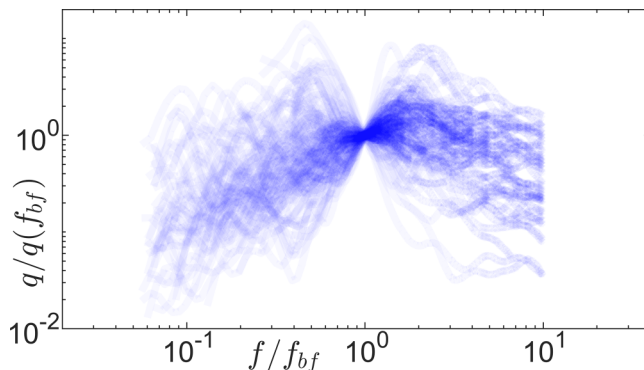


FIG. 6. Overplot of turbulent power density profiles with $\frac{f_g - f_b}{f_g} < 1$.

B. Turbulent power density outside of the plasma disk

Turbulent power in nightside Jupiter's magnetosphere calculated with Eq. (18) from magnetometer measurements on Juno spacecraft are shown in Fig. 7. Turbulent power values are calculated in MHD subrange from 10 min intervals and then averaged along all measured local time. In this study break in the power spectrum is determined by a curve fitting routine independently from calculation of gyrofrequency [Figs. 2(b), 2(c), and 3]. So as sampling moves from inside of the plasma disk to the outside, power spectrum unbends and the full range of sampling frequencies is used as MHD subrange.

Turbulent power density is distributed nonuniformly in Jupiter's magnetosphere. Higher power density measurements near the middle of the plasma disk (Figs. 4 and 7) point to that this is where turbulent power is introduced. Energy is then transferred outside of the plasma disk with shear Alfvén waves dissipating out of the system along the way. Figure 7 also shows some active areas outside of the plasma disk. Equation (18) is sensitive to the estimate of ρ . In this a study model of density distribution from Ref. [13] is used. If, however, there are pockets of plasma with increased magnetic activity outside of the plasma disk, where it is not anticipated by the model, then these areas will light up due to the overestimate of v'_A . A more thorough study in conjunction with plasma instruments on Juno spacecraft can potentially point to transport mechanisms outside of the plasma disk. This, however, is outside of the scope of this paper.

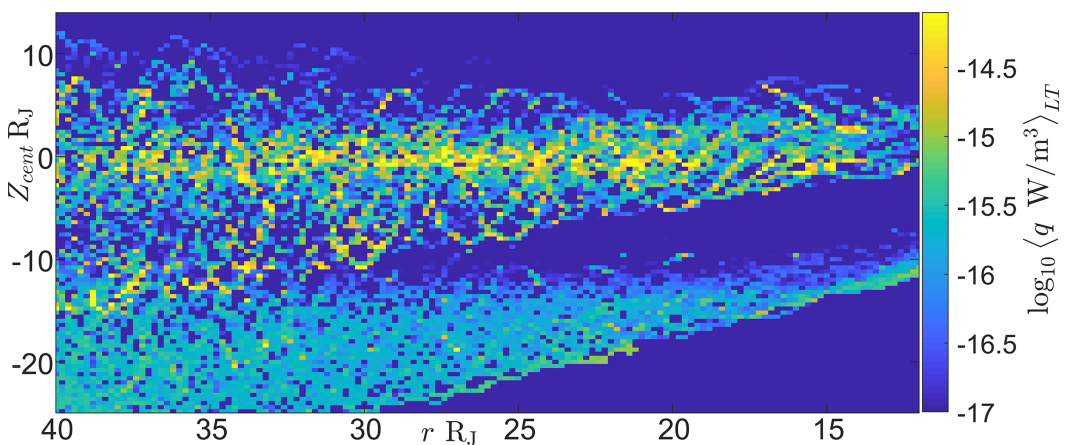


FIG. 7. Radial profile of turbulent power density in MHD subrange inside and outside of the plasma disk calculated with Eq. (18).

X. DISCUSSION

Turbulent oscillations were suggested as a mechanism for increase of plasma fluid temperature in plasma disks of Jovian planets. In this study, the plausibility of heating of heavy-ion dense plasma in presence of a strong magnetic field with turbulent oscillations was examined. Relation of ion velocity variations and fluctuations in the magnetic field was derived for MHD and kinetic subranges. This was then used to determine turbulent power density in the magnetic field and plasma fluid system. Magnetometer data from Juno mission to Jupiter was used to demonstrate turbulent power in MHD and kinetic subranges. Extensive map of turbulent activity in Jupiter's night side magnetosphere is presented.

In this work interdependence of ion motion variations with magnetic field fluctuations for heavy-ion dense plasma in MHD subrange was shown from magnetohydrodynamic principles. It was also demonstrated that in the kinetic subrange velocity variations and field fluctuations disassociate. Heavy-ion velocity variations decay rapidly at frequencies higher than the gyrofrequency and turbulent power is mostly contained in fluctuations of the magnetic field. So that critical balance argument [14] does not have a physical meaning at frequencies higher than the gyrofrequency.

This study shows that perpendicular field fluctuations generate ion velocity variations parallel to the main magnetic field through radiation pressure by inducing perpendicular electric field oscillations. These variations, however, scale as $(\frac{v_A}{c})^2$ so that perpendicular magnetic field variations can generate helixlike oscillations in electron or maybe even in light-ion plasma, however, in heavy-ion dense plasma in MHD subrange parallel velocity variations generated by radiation pressure are negligible.

Interestingly the decay dynamics of δv_{\parallel} are opposite to that of δv_{\perp} . Parallel velocity variations decay more rapidly in the MHD than in the kinetic subrange. In fact in the kinetic subrange once frozen-in approximation no longer applies, decay in motion due to radiation pressure with increase in frequency is comparable to decay of shear motion in the MHD subrange. In case of shear Alfvén wave turbulence, δv_{\parallel} terms have negligible amplitudes near gyration scales so that shallower decay in the kinetic subrange will not do much to improve plasma heating. However, the step up in velocity amplitudes near gyration scales (not letting them to decay in MHD subrange) will allow shear wave turbulence process to keep energy in the plasma fluid via parallel velocity variations letting it to cascade down scales, heating ions.

Use of counterpropagating waves to heat plasma fluid was examined. This study shows that in the case of interaction of waves with the same linear polarization, turbulent power in the kinetic subrange is contained in the magnetic field with rapid decay of ion velocity variations in the kinetic subrange. However, interaction of waves with opposite linear polarization results in turbulent power to be carried by the plasma fluid instead. The challenge is that along the cascade through different scales different linear polarization modes will be mixed, which will result in sporadic increases and decreases of vorticity and ion velocity variations in the kinetic subrange.

Turbulent power in Jupiter's night side magnetosphere was observed from magnetometer measurements on the Juno mission. Observations of break frequency in the power spectrum of moving plasma point to that fluctuations at gyrofrequencies can play an important role in converting kinetic energy of plasma flow into thermal [8]. Examination of turbulent power density across MHD and kinetic subranges in Jupiter's magnetosphere demonstrate that cases with the observed break in power spectrum similar to gyrofrequency indeed correspond with an increase in observed power density near break frequency. This study shows that in heavy-ion dense plasma fluid turbulent oscillations by themselves are not good candidates for plasma heating mechanism. However, fluctuations at frequencies near break and gyrofrequencies play an important role in plasma heating.

Detailed radial map of turbulent power is presented. Observations show that power density is higher in the plasma disk, indicating that turbulent fluctuations are generated within the plasma fluid. Turbulent power then travels out of the plasma disk via shear Alfvén waves, dissipating out of the system along the way.

ACKNOWLEDGMENT

This work is supported by NASA Grant No. 80NSSC20K1279.

-
- [1] A. J. Chorin, *Vorticity and Turbulence* (Springer Science & Business Media, Berlin, 2013), Vol. 103.
 - [2] P. Delamere, C. Ng, P. Damiano, B. Neupane, J. Johnson, B. Burkholder, X. Ma, and K. Nykyri, Kelvin–helmholtz-related turbulent heating at saturn’s magnetopause boundary, *J. Geophys. Res.: Space Phys.* **126**, e2020JA028479 (2021).
 - [3] C. Ng, P. Delamere, V. Kaminker, and P. Damiano, Radial transport and plasma heating in Jupiter’s magnetodisc, *J. Geophys. Res.: Space Phys.* **123**, 6611 (2018).
 - [4] W. Baumjohann and R. Treumann, *Basic Plasma Space Physics* (Imperial College Press, London, 1996).
 - [5] J. D. Jackson, *Classical Electrodynamics* (Wiley, New York, 1999).
 - [6] A. Hasegawa, Particle acceleration by mhd surface wave and formation of aurora, *J. Geophys. Res.* **81**, 5083 (1976).
 - [7] A. Mangeney, C. Lacombe, M. Maksimovic, A. Samsonov, N. Cornilleau-Wehrin, C. Harvey, J.-M. Bosqued, and P. Trávníček, Cluster observations in the magnetosheath—part 1: Anisotropies of the wave vector distribution of the turbulence at electron scales, in *Annales Geophysicae* (Copernicus Publications, Göttingen, 2006), Vol. 24, pp. 3507–3521.
 - [8] V. Kaminker, On asymmetry of magnetic activity and plasma flow temperature in Jupiter’s magnetosphere, *Sci. Rep.* **13**, 16311 (2023).
 - [9] A. N. Kolmogorov, The local structure of turbulence in incompressible viscous fluid for very large Reynolds numbers, *Proceedings of the Royal Society of London. Series A: Mathematical and Physical Sciences* **434**, 9 (1991).
 - [10] R. M. Rosa, *Turbulence Theories* (Elsevier, Amsterdam, 2006).
 - [11] J. Saur, Turbulent heating of Jupiter’s middle magnetosphere, *Astrophys. J.* **602**, L137 (2004).
 - [12] L. Cheng, Y. Lin, J. Perez, J. R. Johnson, and X. Wang, Kinetic Alfvén waves from magnetotail to the ionosphere in global hybrid simulation associated with fast flows, *J. Geophys. Res.: Space Phys.* **125**, e2019JA027062 (2020).
 - [13] F. Bagenal and P. A. Delamere, Flow of mass and energy in the magnetospheres of Jupiter and Saturn, *J. Geophys. Res.: Space Phys.* **116**, A5 (2011).
 - [14] P. Goldreich and S. Sridhar, Toward a theory of interstellar turbulence. 2: Strong Alfvénic turbulence, *Astrophys. J.* **438**, 763 (1995).
 - [15] D. Biskamp, E. Schwarz, and J. F. Drake, Two-dimensional electron magnetohydrodynamic turbulence, *Phys. Rev. Lett.* **76**, 1264 (1996).
 - [16] J. Cho and A. Lazarian, The anisotropy of electron magnetohydrodynamic turbulence, *The Astrophys. J.* **615**, L41 (2004).
 - [17] P. Phipps and F. Bagenal, Centrifugal equator in Jupiter’s plasma sheet, *J. Geophys. Res.: Space Phys.* **126**, e2020JA028713 (2021).
 - [18] F. Bagenal, Planetary magnetospheres, *Plan. Stars Stellar Syst.* **3**, 251 (2013).
 - [19] J. Connerney, M. Benn, J. Bjarno, T. Denver, J. Easley, J. Jorgensen, P. Jorgensen, P. Lawton, A. Malinnikova, J. Merayo *et al.*, The juno magnetic field investigation, *Space Sci. Rev.* **213**, 39 (2017).
 - [20] C. Tao, F. Sahraoui, D. Fontaine, J. de Patoul, T. Chust, S. Kasahara, and A. Retinò, Properties of Jupiter’s magnetospheric turbulence observed by the Galileo spacecraft, *J. Geophys. Res.: Space Phys.* **120**, 2477 (2015).
 - [21] R. J. Leamon, C. W. Smith, N. F. Ness, and H. K. Wong, Dissipation range dynamics: Kinetic Alfvén waves and the importance of β_e , *J. Geophys. Res.* **104**, 22331 (1999).
 - [22] V. Kaminker, P. Delamere, C. Ng, T. Dennis, A. Otto, and X. Ma, Local time dependence of turbulent magnetic fields in Saturn’s magnetodisc, *J. Geophys. Res.: Space Phys.* **122**, 3972 (2017).